

Oriented Gradient Histogram applied to P300 Detection

Rodrigo Ramele^{1,*}, Ana Julia Villar¹ and Juan Miguel Santos¹

¹ Computer Engineering Department, Instituto Tecnológico de Buenos Aires (ITBA); info@itba.edu.ar

* Correspondence: rramele@itba.edu.ar; Tel.: +54-11-2150-4800(5834)

† Current address: C1437FBH Lavarden 315, Ciudad Autónoma de Buenos Aires, Argentina

Academic Editor: name

Version December 1, 2017 submitted Typeset by L^AT_EX

Abstract: The analysis of Electroencephalographic (EEG) signals is of ulterior importance to elucidate patterns that could improve the implementation of Brain Computer Interfaces (BCI). These systems are meant to provide alternative pathways to transmit volitional information which could potentially enhance the quality of life of patients affected by neurodegenerative disorders or improve Human Computer Interaction systems. Of particular interests are those which are based on the recognition of Event-Related Potentials (ERP) because they can be elicited by external stimuli and used to implement spellers, to control external devices or even avatars in virtual reality environments. This work mimics what electroencephalographers have been doing clinically, visually inspecting and categorizing phenomena within the EEG by the extraction of features from the images of the plots of the signals. It also aims to provide a framework to analyze, characterize and classify EEG signals, with a focus on the P300, an ERP elicited by the oddball paradigm of rare events. The validity of the method is shown by offline processing a public dataset of Amyotrophic Lateral Sclerosis (ALS) patients.

Keywords: electroencephalography (EEG); BCI; P300; ALS; NBN; HOG; SIFT

0. Introduction

Although recent advances in neuroimaging techniques (particularly radio-nuclear and radiological scanning methods) [1] have diminished the prospects of the traditional Electroencephalography (EEG), the advent and development of digitalized devices has pressed for a revamping of this hundred years old technology. Their versatility, ease of use, temporal resolution, ease of development and fabrication, and its proliferation as consumer devices, are pushing EEG to become the de-facto non invasive portable or ambulatory method to access and harness brain information [2]

A key contribution to this expansion has been the field of Brain Computer Interfaces (BCI) [3] which is the pursuit of the development of a new channel of communication particularly aimed to persons affected by neurodegenerative diseases.

One noteworthy aspect of this novel communication channel is the ability to volitionally transmit information from the Central Nervous System (CNS) to a computer device and from there use that information to control a wheelchair [4], as input to a speller application [5], in a Virtual Reality environment [6] or as aiding tool in a rehabilitation procedure [7]. The holy grail of BCI is to implement a new complete and alternative pathway to restore lost locomotion [3].

EEG signals are remarkably complex and have been characterized as a multichannel non-stationary stochastic process. Additionally, they have high variability between different subjects and even between different moments for the same subject, requiring adaptive and co-adaptive calibration and learning procedures [8]. Hence, this imposes an outstanding challenge that is necessary to overcome in order to extract information from raw EEG signals.

Moreover, EEG markers [8] that can be used to volitionally transmit information are limited, and each one of them has a particular combination of appropriate methods to decode them. Inevitably, it

is necessary to implement distinct and specialized algorithmic methods, to filter the signal, enhance its Signal to Noise Ratio (SNR), and try to determine some meaning out of it.

BCI has gained mainstream public awareness with worldwide challenge competitions like Cybathlon [9] and even been broadcasted during the inauguration ceremony of the 2014 Soccer World Cup. New developments have overcome the out-of-the-lab high-bar and they are starting to be used in real world environments [10]. However, they still lack the necessary robustness, and its performance is well behind any other method of human computer interaction, including any kind of detection of residual muscular movement [8].

In this work, a new method to characterize and classify EEG signals is presented, expanded and detailed. Its validity is verified by processing offline data for ALS patients. This is the continuation of the work previously presented in [11], where it was applied to rhythmic patterns, and that it can be extended to describe transient events like those produced by P300 Event Related Potential [12].

The method is based on the morphological analysis of the shape of the EEG signal [13,14] and was inspired by mimicking what traditionally electroencephalographers have been performing for almost a century: visually inspecting raw signal plots [15].

This paper reports a method to, (1) characterize EEG signals based on the identification of their structure in the shape domain using histograms of oriented gradients extracted from the image of signal plots, and (2) how this characterization can be used to implement a BCI classification scheme to identify Event Related Potentials, particularly the well-known P300, on an offline and public dataset.

This article unfolds as follows: in Section 1.1 the Feature Extraction based on Histogram of Gradients of the Signal Plot method is explained. Section 1.1.1 and 1.1.2 describe the processing pipeline. Section 1.1.3 clarifies how the image of the signal plot is constructed whereas Section 1.1.4 describes in detail the feature extraction procedure. Section 1.1.5 presents the classification algorithm based on Naive Bayes Near Neighbor and the final Section shows results and discussion where we expose our remarks, conclusions and future work.

1. Materials and Methods

1.1. Feature Extraction based on Histogram of Gradients of the Signal Plot

The P300 [12,16] is a positive deflection of the EEG signal which occurs around 300 ms after the onset of a rare and deviant stimulus that the subject is expected to attend. It is produced under the oddball paradigm [3] and though it is consistent across different subjects. It has a lower amplitude ($\pm 5\mu V$) compared to basal EEG activity, reaching a SNR of around -15 db estimated based on the amplitude of the P300 response signal divided by the standard deviation of the background EEG activity [17]. This signal can be used to implement a speller application by means of a Speller Matrix [16]. Fig. 1 shows an example of a Speller Matrix used in the OpenVibe Open Source software [18], where the flashings of rows and columns provide the deviant stimulus required to elicit this physiological response. Each time a row or column that contains the desired letter flashes, the corresponding synchronized EEG signal should also contain the P300 signature and by detecting it, the selected letter can be identified.

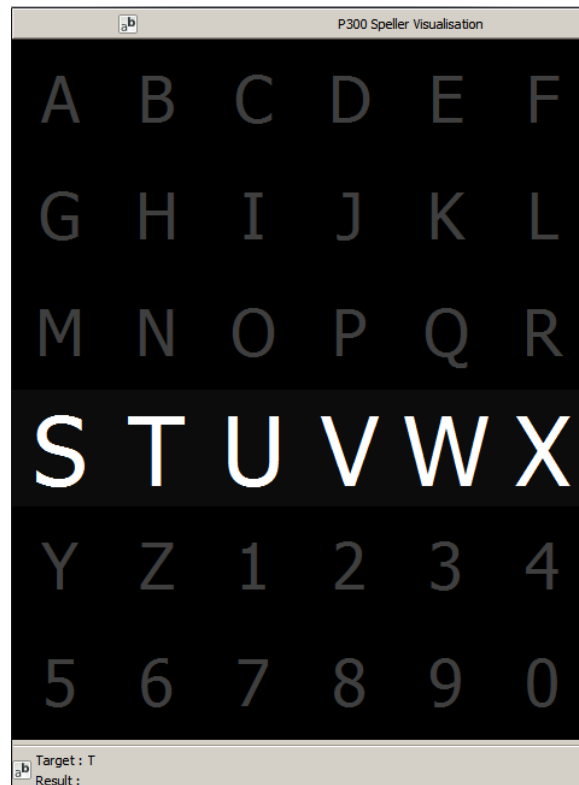


Figure 1. Example of a Speller Matrix. Rows and columns flash intermittently in random permutations.

1.1.1. Preprocessing

The first step consists of the enhancement of the SNR of the P300 pattern above the level of basal EEG. The processing pipeline starts by applying a notch filter to the raw signal, a 4th degree 10 Hz lowpass Butterworth filter and finally a decimation with an Finite Impulse Response (FIR) filter of order 30 from the original sampling frequency down to 16 Hz [19].

1.1.2. Processing Pipeline

- **Artefact Removal:** The EEG signal matrix is processed on a channel by channel basis. For every 12 flashing stimuli, i.e. one complete sequence of intensification of each of the 6 rows plus the 6 columns, a basic artefact elimination procedure is implemented by removing the entire segment when any signal deviates above/below $\pm 70\mu V$.
- **Segmentation:** For each of the 12 stimuli, a window of 1 second of the multichannel signal is extracted, starting from the stimulus onset, corresponding to each row/column intensification. Two of these segments are labeled as *hit*, whereas the remaining 10 are labeled as *no hit*. A hit represents that the EEG segment should contain the P300 ERP signature time-locked to the flashing stimulus.
- **Signal Averaging:** The P300 ERP is deeply buried under background EEG so the traditional approach to identify it is by point-to-point averaging the time-locked stacked signal segments. Hence the values which are not related to, and not time-locked to the onset of the stimulus are canceled out [20].

This last step determines the operation of any P300 Speller. In order to obtain an improved signal in terms of its SNR, repetitions of the sequence of row/column intensification are necessary. And, at the same time, as long as more repetitions are needed, the ability to transfer information faster is diminished, so there is a trade-off that must be acutely determined.

1.1.3. Signal Plotting

The underlying idea of this method is to generate a template for the signal [11], based on the image plot. Hence, the first step is its transformation into a temporary binary image.

The signal is first scaled and standardized (i.e. z-score) by

$$\tilde{x}(t, c) = \left\lfloor \gamma \cdot \frac{(x(t, c) - \bar{x}(c))}{\sigma(c)} \right\rfloor \quad (1)$$

where γ is the image scale, t is the time and $x(t, c)$ is the point-to-point averaged EEG matrix defined for each t and for a channel c . Lastly, $\bar{x}(c)$ and $\sigma(c)$ are the mean and standard deviation of x .

Consequently, the image is constructed by placing the sample points according to

$$I(z_1, z_2) = \begin{cases} 255 & \text{if } z_1 = \gamma \cdot t; z_2 = \tilde{x}(t, c) + z(c) \\ 0 & \text{otherwise} \end{cases} \quad (2)$$

where z_1 and z_2 iterate over the width (based on the length of the signal segment) and height (based on the peak-to-peak amplitude) of the newly created image. The function $z(c)$ is the *zerolevel* which is the location on the image where the signal's zero value should be located in order to fit the entire signal within the image:

$$z(c) = \left\lfloor \frac{\max \tilde{x}(t, c) - \min \tilde{x}(t, c)}{2} \right\rfloor - \left\lfloor \frac{\max \tilde{x}(t, c) + \min \tilde{x}(t, c)}{2} \right\rfloor \quad (3)$$

In order to complete the plot from the pixels, the Bresenham [11,21] algorithm is used to interpolate straight lines between each pair of consecutive pixels.

1.1.4. Feature Extraction: Histogram of Oriented Gradients

On the generated image, a keypoint \mathbf{kp} is placed on a pixel (x_{kp}, y_{kp}) over the image plot and a window around the keypoint is considered. A local image patch is constructed by dividing the window in 16 blocks of size $3s$ each one, where s is the scale of the local patch and it is an input parameter of the algorithm. It is arranged in a 4×4 grid and the pixel \mathbf{kp} is the patch center.

A local representation of the shape of the signal within the patch can be described by obtaining the gradient orientations on each of the 16 blocks and creating a histogram of gradients. This technique is based on Lowe's SIFT [22] method, and it is biomimetically inspired in how the visual cortex detects shapes by analyzing orientations. In order to calculate the histogram, the interval $[0 - 360]$ of possible angles is divided in 8 bins, each one at 45 degrees. For each spacial bin $i, j = \{1, 2, 3, 4\}$, corresponding to the indexes of each block $B_{i,j}$, the orientations are accumulated in a 3-dimensional histogram h through the following equation:

$$h(\theta, i, j) = 3s \sum_{\mathbf{x} \in B_{i,j}} w_{\text{ang}}(\angle J(\mathbf{x}) - \theta) w_{ij} \left(\frac{\mathbf{x} - \mathbf{kp}}{3s} \right) |J(\mathbf{x})| \quad (4)$$

where $\theta \in \{0, 45, 90, 135, 180, 225, 270, 315\}$, $i, j \in \{1, 2, 3, 4\}$, $|J(\mathbf{x})|$ is the norm of the gradient vector found at each block of the patch using finite differences, $\angle J(\mathbf{x})$ is the angle of the gradient vector, θ is the angle bin, \mathbf{x} is a pixel from the i, j -block $B_{i,j}$ and $w_{\text{ang}}(\cdot)$ and $w_{ij}(\cdot)$ are linear interpolation functions used by Lowe and Vedaldi et al. in [22,23]. Lastly, the fixed value of 3 is a magnification factor which corresponds to the number of pixels per each block when $s = 1$. As the patch is of size 4×4 and 8 bin angles are considered, a descriptor of 128 dimension is obtained. It can be observed that in each step, the histogram is computed by multiplying by $|J(\mathbf{x})|$, so the method considers both, the magnitude and the orientation of the gradient vector.

Fig. 2 shows an example of a patch and a scheme of the histogram computation. Fig. 2(a) is a plot of the signal and the patch centered in the keypoint. In Fig. 2(b) the possible orientations on each patch are illustrated. They form the corresponding \mathbf{kp} -descriptor of 128 coordinates. The first two

135 blocks orientations are shown. Following this procedure for every assigned keypoint, we obtain N_{kp}
 136 descriptors.

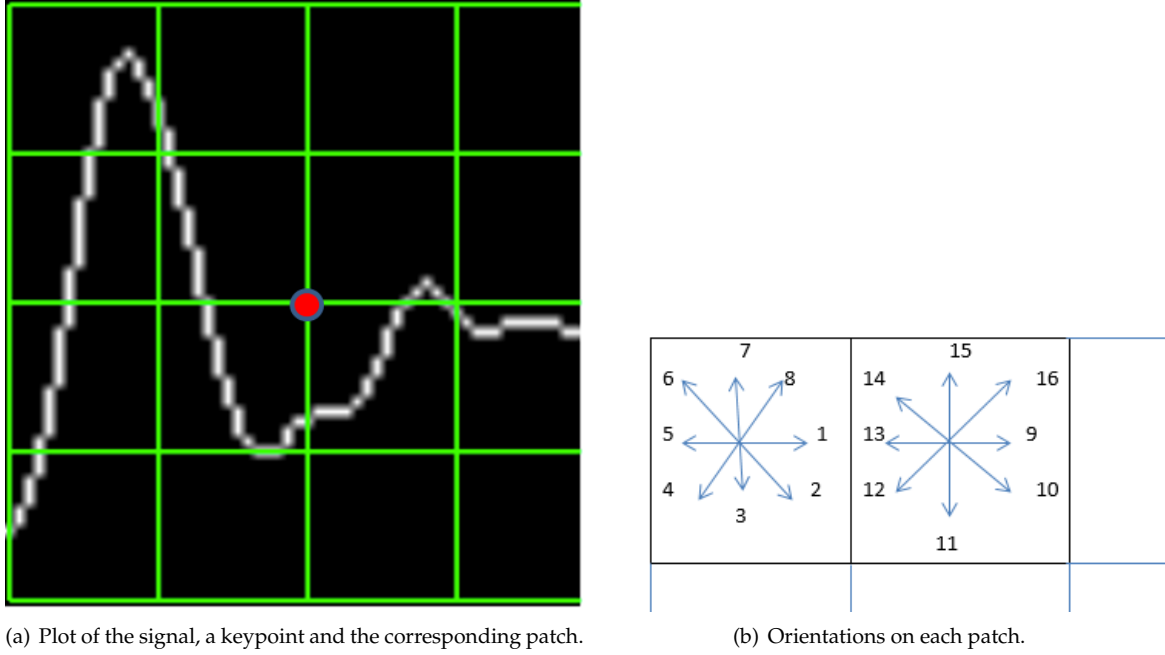


Figure 2. Example of a patch and a scheme of the orientations histogram computation.

137 1.1.5. Classification

138 The following step is classify the descriptors $\{d_{kp}, kp = 1, \dots, 12\}$ in order to determine the
 139 correct row and column of the chosen letter en the Speller Matrix. The classification is carried out
 140 by using a discriminative semi-supervised classification method, based on the Naive Bayes Nearest
 141 Neighbor (NBNN) [24].

142 The aim is to identify the selected letter from the matrix. Previously, during training phase,
 143 descriptors from labeled segments are extracted. The P300 templates are grouped in a template set
 144 called T . Rows are labeled 1-6, whereas columns are labeled 7-12. The process has the following steps:

- 145 1. Highlight randomly the rows and columns from the matrix. There are one row and one column
 146 that matches the selected letter by the user.
- 147 2. For $k = 1 - 6$: Obtain the descriptor from the image of the signal plot according to the method
 148 described in Section 1.1.4, d_1^r, \dots, d_6^r for rows and d_1^c, \dots, d_6^c .
- 149 3. For $k = 7 - 12$: Compute

$$\hat{r} = \arg \min_u \sum_{q \in NN_T(d_u^r)} \|q - d_u^r\|^2, u = 1, \dots, 6 \quad (5)$$

150 This procedure is repeated for the 6 columns.

$$\hat{c} = \arg \min_u \sum_{q \in NN_T(d_u^c)} \|q - d_u^c\|^2, u = 7, \dots, 12 \quad (6)$$

151 While doing classification based on local features, which encode partial information, one
 152 problem that frequently arises is how to ensemble the individual classification of each local
 153 characteristic to the whole image.

The NBNN algorithm tackles this problem by comparing each image against a whole classification class. It is characterized by the set of descriptors closest to each one of the descriptors obtained for the query image. The algorithm find the predicted class \hat{C} of a query image by means of the following minimization:

$$\hat{C} = \arg \min_C \sum \|d_i - NN_C(d_i)\|^2 \quad (7)$$

where C is the a class, d_i is a descriptor that belongs to the query image and $NN_C(d_i)$ is the corresponding near neighbor descriptor for the class C .

This basic method was adapted to the P300 Speller and the classifier works according to the following modified equation:

$$\hat{Q}_{rc} = \arg \min_q \sum_{x_i \in NN_T^k(q)} \|x_i - q\|^2 \quad (8)$$

The first step consists in extracting labeled *hit* descriptors from the training set which are thus grouped together in a KD-tree [23] template set T . On decoding stage, 12 new images from the signal segments are generated, and their descriptors extracted. The 12 descriptors are divided in rows and columns. For each one of the 6 query descriptors q for row/column, its k nearest neighbours in the template set T , $NN_T^k(q)$ (acquired during the training phase) are obtained and the distance between each one of them, x_i , and the query descriptor q is summarized. The query descriptor q that minimizes this summation is the one that is chosen, first among the 6 rows, and then among the remaining 6 columns. By performing this procedure, the correct letter can be identified by matching the row r and column c from the P300 speller matrix.

Especially in the case of the P300 response, the oddball paradigm requires that one of the stimuli need to be infrequent so that will unavoidably force the data to be unbalanced [25]. The NBNN method suffers from biased classification on unbalanced classes [26]. By reversing the roles of the query and the class in Eq. 8, it is only necessary to obtain the template set T with the learned descriptors representative of the P300 ERP, hence avoiding the problem of unbalanced classes.

1.2. Experimental Protocol

To verify the validity of the proposed framework and method, the public dataset 008-2014 [27] published on the BNCI-Horizon website [28] by IRCCS Fondazione Santa Lucia, was used to perform an offline BCI Simulation to decode the spelled words from the provided signals. The algorithm was implemented using VLFeat [23] Computer Vision libraries on MATLAB 2014a (Mathworks Inc., Natick, MA, USA).

1.2.1. P300 ALS Public Dataset

The experimental protocol used to generate this dataset is explained in [27] but can be summarized as follows: 8 subjects with confirmed diagnoses but on different stages of ALS disease, were recruited and accepted to perform the experiments. The P300 detection task designed for this experiment consisted of spelling 7 words (runs) of 5 letters each, using the traditional P300 Speller Matrix [16] where the flashings of rows and columns provide the deviant stimulus required to elicit this physiological response. The first 3 runs were used for training and the remaining 4 for testing with visual feedback. A trial, as defined by the BCI2000 platform [29], was every attempt to select a letter from the speller, and it was composed of signal segments corresponding to 10 repetitions of flashes of 6 rows and 6 columns of the traditional 6x6 P300 matrix, yielding 120 repetitions. Flashing of row/columns was performed for 0.125 s, following by a resting period (i.e. Inter-stimulus interval) of the same length. After 120 repetitions an inter-trial pause was included before resuming with the following letter.

The recorded dataset was sampled at 256 Hz and consisted of an EEG matrix for electrode channels Fz,Cz,Pz,Oz,P3,P4,PO7 and PO8, identified according to the 10-20 International System, for each one of the 8 subjects.

In order to asses and verify the identification of the P300 response, subjects are instructed to perform a copy-spelling task where they have to fix their attention to successive letters in order to copy a previously determined set of words (in contrast to an online free-running operation of the speller where each users decides on its own what letter to choose).

1.2.2. Parameters

Parameters were selected according to the experimental protocol. As the P300 event latency and amplitude vary greatly between subjects, it is necessary to provide a patch that will be able to capture an entire transient event. Equations 9 and 10 can be used to map the original signal parameters to local image patch structure.

$$s = \frac{\Delta\mu V}{4 \cdot 3} \cdot \gamma \quad (9)$$

$$s = \frac{\lambda \cdot Fs}{4 \cdot 3} \cdot \gamma \quad (10)$$

where Fs is the sample frequency of the EEG signal (downsampled to 16 Hz), λ is the length in seconds covered by the patch, and $\Delta\mu V$ corresponds to the amplitude in microvolts that can be covered by the height of the patch. By using $s = 3$ and a quadruple scale of the image $\gamma = 4$ this gives the local patch, and the descriptor, the ability to identify events of $9 \mu V$ of amplitude, a resolution of $1 \text{ Pixel} = \frac{1}{4} \mu V$ and span of $\lambda = 0.56s$ (because the patch is a geometric square, s must be the same to map both the height and the required span of the signal). Finally, descriptor locations T were selected at $x = 0.55s \cdot Fs \cdot \gamma = 35$ and $y = z(c)$ (Eq. 3).

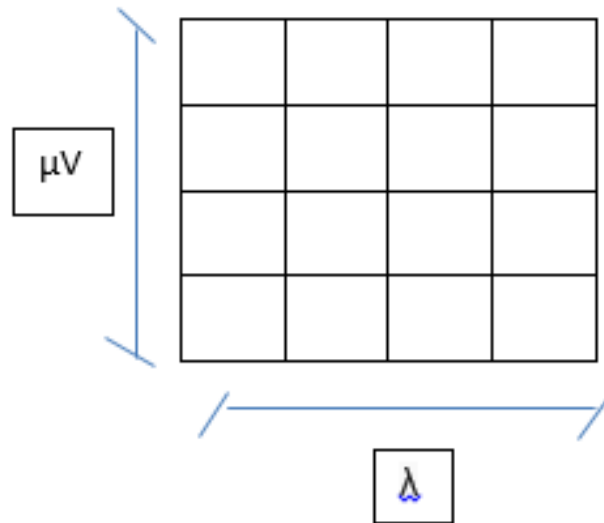


Figure 3. The local patch captures the signal information based on both the vertical and horizontal scale.

1.2.3. P300 for healthy subjects

We replicated the same experiment on healthy subjects using g.Tec g.Nautilus 8 channels, bla bla bla bla in order to validate the obtained results.

2. Results and Discussion

In Figure 4 the grand average (point-to-point) for all the subjects using the information from all the segments can be shown. The P300 characteristic curve can be seen particularly in subjects 2, and 6 and in a lesser extend in the remaining subjects. In order to correctly decode the selected letter from each trial, particular care was observed to avoid unbalanced number of epochs (i.e. an unequal number of epochs on each condition), because that may introduce bias in the classification procedure (the variance of averaged signals is inversely proportional to the number of samples and the procedure would be discriminating signals with different variances).

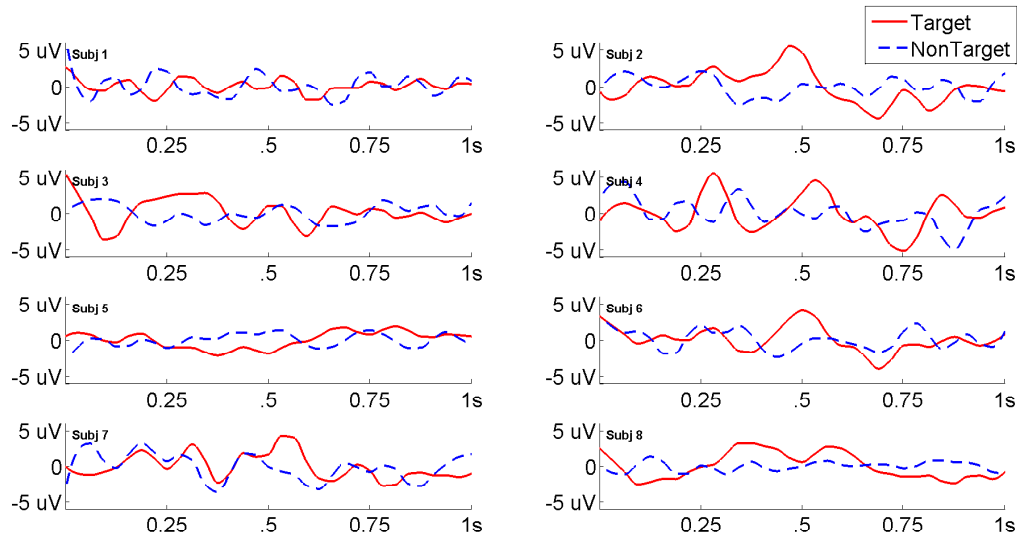


Figure 4. Point-to-point grand averages of epochs obtained for hits (solid line) and no hits (dashed line) for each one of the 8 subjects for channel Cz. The P300 characteristic curve can be well identified particularly on subjects 2 and 6.

Results are shown in Table 1 where the percentage of correctly spelled letters is calculated while performing an offline BCI Simulation. From the 7 trials for each subject, the first 3 were used as training, and the remaining 4 for testing. The best performing channel is informed as well. It is of particular interest that using this method, the best performing channel was not always Cz, and instead occipital channels PO8 and PO7 showed higher performances [7,10].

Table 1. Percentage of correctly predicted letters while performing an offline BCI Simulation for the best performing channel for each subject. Chance level is 0.02

Participant	BPC	Performance
1	Cz	0.35
2	Fz	0.85
3	Cz	0.25
4	PO8	0.55
5	PO7	0.40
6	PO7	0.60
7	PO8	0.80
8	PO7	0.95

The ITR, or BTR, in the case of reactive BCIs [3] strongly depends on the amount of signal averaging required to transmit a valid and robust selection. The Performance curves (Fig. 5) show

232 how the percentage of correctly identified letters depends on the number of repetitions that were used
 233 to obtain the averaged signal.

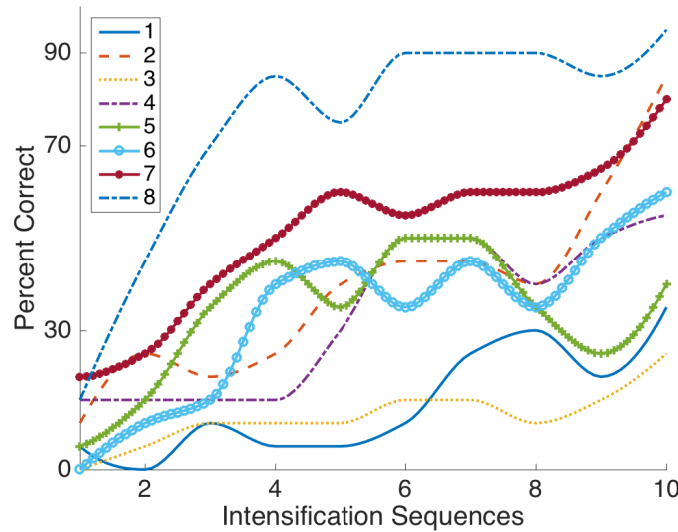


Figure 5. Performance curves for the eight subjects included in the published dataset. Three out of eight subjects achieved the necessary performance to implement a valid P300 speller.

234 We found that only by using the visual aspect of the P300 signal plot, for some subjects it was not
 235 possible to find templates that could allow the classification to reach a higher level. We hypothesize
 236 that as subjects may have different latencies and amplitudes of the P300 signal [27], it may also be the
 237 case that the shape of the generated ERP may vary greatly in an intra-subject manner, thus the pattern
 238 could not be well generalized and a higher performance could not be reached (Fig. 6).

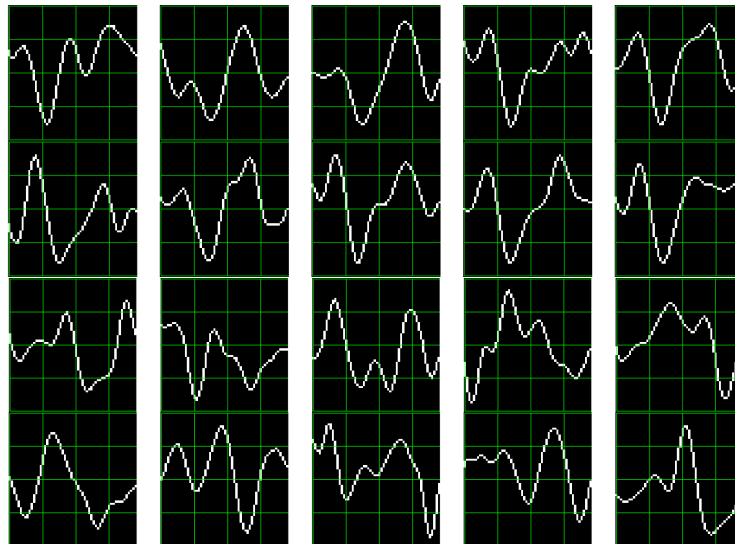


Figure 6. Ten P300 template patches found for subjects 8 (up) and 3(down). In coincidence with the performance results, the P300 signature is more clear and consistent for subject 8 (higher performance) while for subject 3 (lower performance) the characteristic pattern is much more difficult to perceive.

3. Conclusion

A method to characterize and classify EEG signals where their characterization is transient in time-space, like the P300 ERP, has been presented.

The adaptive behaviour of the algorithm make it well suited when the shape of the pattern elicited by the P300 response does not conform to the predicted structure. This is due to the fact that the descriptors are directly based on how the signals behave in shape domain (i.e. *how actually they looked like*) for the training and calibration step, and they do not require any prior knowledge about the signal. In contrast, when the shape of the ERP response is not consistent across the same subject, this method would not be able to find the templates and speller performance could be penalized.

At the same time, by analyzing the generated descriptors, which map in a very detailed and synthetic structure the shape information contained within the patch, a metric about the consistency of the shape of the generated P300 response could also be derived. It may be worthy of further consideration to evaluate if there is any correlation between the lower performance obtained for some subjects and the characterization of their ALS stage.

We believe that the expanding and the understanding of this tool in order to automatically classify those patterns in EEG that are specifically identified by their shapes (e.g. K-Complex, Vertex Waves, Positive Occipital Sharp Transient [15]) is a prospect future work to be considered. It may also provide assistance to physician or electroencephalographers to help them locate these EEG patterns particularly in long recording periods, frequent in sleep research.

Moreover, this method can be used as an alternate *BCI predictor* [8], i.e. to detect BCI illiteracy or to predict the achievable performance of a given method, or even as a tool for artefact removal (which is performed on many occasions by visually inspecting the signal).

Acknowledgments: This project was supported by the ITBACyT-15 funding program issued by ITBA University.

Conflicts of Interest: The authors declare that there is no conflict of interest regarding the publication of this article.

Abbreviations

The following abbreviations are used in this manuscript:

EEG: Electroencephalography

BCI: Brain Computer Interfaces

SNR: Signal to Noise Ratio

CNS: Central Nervous System

ALS: Amyotrophic Lateral Sclerosis

ERP: Event-Related Potential

P300: Positive deflection of an Event-Related Potential which occurs 300 ms after onset of stimulus

ITR: Information Transfer Rate

BTR: Bit Transfer Rate

SIFT: Scale Invariant Feature Transform

NBNN: Naive Bayes Nearest Neighbor

HOG: Histogram Of Gradients

Bibliography

- Schomer, D.L.; Silva, F.L.D. *Niedermeyer's Electroencephalography: Basic Principles, Clinical Applications, and Related Fields*; Walters Klutter -Lippincott Williams & Wilkins, 2010.
- De Vos, M.; Debener, S. Mobile EEG: Towards brain activity monitoring during natural action and cognition. *International Journal of Psychophysiology* **2014**, *91*, 1–2.
- Wolpaw, J.; E., W. *Brain-Computer Interfaces: Principles and Practice*; Oxford University Press, 2012.

4. Carlson, T.; del R. Millan, J. Brain-Controlled Wheelchairs: A Robotic Architecture. *IEEE Robotics & Automation Magazine* **2013**, *20*, 65–73.
5. Guger, C.; Daban, S.; Sellers, E.; Holzner, C.; Krausz, G.; Carabalona, R.; Gramatica, F.; Edlinger, G. How many people are able to control a P300-based brain-computer interface (BCI)? *Neuroscience Letters* **2009**, *462*, 94–98.
6. Lotte, F.; Faller, J.; Guger, C.; Renard, Y.; Pfurtscheller, G.; Lécuyer, A.; Leeb, R., Combining BCI with Virtual Reality: Towards New Applications and Improved BCI. In *Towards Practical Brain-Computer Interfaces: Bridging the Gap from Research to Real-World Applications*; Springer Berlin Heidelberg: Berlin, Heidelberg, 2013; pp. 197–220.
7. Jure, F.; Carrere, L.; Gentiletti, G.; Tabernig, C. BCI-FES system for neuro-rehabilitation of stroke patients. *Journal of Physics: Conference Series* **2016**, *705*, 1–8.
8. Clerc, M.; Bougrain, L.; Lotte, F. *Brain-computer interfaces, Technology and applications 2(Cognitive Science)*; ISTE Ltd. and Wiley, 2016.
9. Riener, R.; Seward, L.J. Cybathlon 2016. *2014 IEEE International Conference on Systems, Man, and Cybernetics (SMC)* **2014**, pp. 2792–2794.
10. Huggins, J.E.; Alcaide-Aguirre, R.E.; Hill, K. Effects of text generation on P300 brain-computer interface performance. *Brain-Computer Interfaces* **2016**, *3*, 112–120.
11. Ramele, R.; Villar, A.J.; Santos, J.M. BCI classification based on signal plots and SIFT descriptors. 4th International Winter Conference on Brain-Computer Interface, BCI 2016; IEEE: Yongpyong, 2016; pp. 1–4.
12. Knuth, K.H.; Shah, A.S.; Truccolo, W.A.; Ding, M.; Bressler, S.L.; Schroeder, C.E. Differentially Variable Component Analysis: Identifying Multiple Evoked Components Using Trial-to-Trial Variability. *Journal of Neurophysiology* **2006**, *95*, 3257–3276.
13. Alvarado-González, M.; Garduño, E.; Bribiesca, E.; Yáñez-Suárez, O.; Medina-Bañuelos, V. P300 Detection Based on EEG Shape Features. *Computational and Mathematical Methods in Medicine* **2016**, pp. 1–14.
14. Yamaguchi, T.; Fujio, M.; Inoue, K.; Pfurtscheller, G. Design Method of Morphological Structural Function for Pattern Recognition of EEG Signals During Motor Imagery and Cognition. Fourth International Conference on Innovative Computing, Information and Control (ICICIC), 2009, pp. 1558–1561.
15. Hartman, a.L. *Atlas of EEG Patterns*; Vol. 65, Lippincott Williams & Wilkins, 2005.
16. Farwell, L.A.; Donchin, E. Talking off the top of your head: toward a mental prosthesis utilizing event-related brain potentials. *Electroencephalography and clinical neurophysiology* **1988**, *70*, 510–23.
17. Hu, L.; Mouraux, A.; Hu, Y.; Iannetti, G.D. A novel approach for enhancing the signal-to-noise ratio and detecting automatically event-related potentials (ERPs) in single trials. *NeuroImage* **2010**, *50*, 99–111.
18. Renard, Y.; Lotte, F.; Gibert, G.; Congedo, M.; Maby, E.; Delannoy, V.; Bertrand, O.; Lécuyer, A. OpenViBE: An Open-Source Software Platform to Design, Test, and Use Brain-Computer Interfaces in Real and Virtual Environments. *Presence: Teleoperators and Virtual Environments* **2010**, *19*, 35–53.
19. Krusienski, D.J.; Sellers, E.W.; Cabestaing, F.; Bayouth, S.; McFarland, D.J.; Vaughan, T.M.; Wolpaw, J.R. A comparison of classification techniques for the P300 Speller. *Journal of Neural Engineering* **2006**, *3*, 299–305.
20. Liang, N.; Bougrain, L. Averaging techniques for single-trial analysis of oddball event-related potentials. *4th International Brain-Computer* **2008**, pp. 1–6.
21. Bresenham, J.E. Algorithm for computer control of a digital plotter. *IBM Systems Journal* **1965**, *4*, 25–30.
22. Lowe, G. SIFT - The Scale Invariant Feature Transform. *International Journal* **2004**, *2*, 91–110.
23. Vedaldi, A.; Fulkerson, B. VLFeat - An open and portable library of computer vision algorithms. *Design* **2010**, *3*, 1–4.
24. Boiman, O.; Shechtman, E.; Irani, M. In defense of nearest-neighbor based image classification. *26th IEEE Conference on Computer Vision and Pattern Recognition, CVPR* **2008**.
25. Tibon, R.; Levy, D.A. Striking a balance: analyzing unbalanced event-related potential data. *Frontiers in psychology* **2015**, *6*, 555.
26. Fornoni, M.; Caputo, B. Scene recognition with naive bayes non-linear learning. *Proceedings - International Conference on Pattern Recognition*, 2014, pp. 3404–3409.
27. Riccio, A.; Simione, L.; Schettini, F.; Pizzimenti, A.; Inghilleri, M.; Belardinelli, M.O.; Mattia, D.; Cincotti, F. Attention and P300-based BCI performance in people with amyotrophic lateral sclerosis. *Frontiers in Human Neuroscience* **2013**, *7*, 732.

- 337 28. Brunner, C.; Blankertz, B.; Cincotti, F.; Kübler, A.; Mattia, D.; Miralles, F.; Nijholt, A.; Ota, B. BNCI
338 Horizon 2020 – Towards a Roadmap for Brain / Neural Computer Interaction. *Lecture Notes in Computer*
339 *Science* **2014**, *8513*, 475–486.
- 340 29. Schalk, G.; McFarland, D.J.; Hinterberger, T.; Birbaumer, N.; Wolpaw, J.R. BCI2000: a general-purpose
341 brain-computer interface (BCI) system. *IEEE transactions on bio-medical engineering* **2004**, *51*, 1034–43.

342 © 2017 by the authors. Submitted for possible open access publication under the terms and conditions of the
343 Creative Commons Attribution (CC-BY) license (<http://creativecommons.org/licenses/by/4.0/>).